

THE THERMOLUMINESCENCE RESPONSE OF
DOPED SILICON DIOXIDE OPTICAL FIBRES TO IONIZING RADIATION

SUHAIRUL HASHIM

A thesis submitted in fulfilment of the
requirements for the award of the degree of
Doctor of Philosophy (Physics)

Faculty of Science
Universiti Teknologi Malaysia

MARCH 2009

I dedicate this work

To my dear parents

Hjh. Sapiah binti Hasan

Hj. Hashim bin Ahmad

Hjh. Fatimah binti Arajol

Hj. Hassan bin Jalani

Whose love, kindness, patience and prayer have brought me this far

To my beloved wife

Sitti Asmah binti Hassan

For her love, understanding and support through my endeavour

To my children

Muhammad Luqmanul Hakim and Farouq Hakimi

Whose presence fills my life with joy

To my siblings

For their endless laughs and tears

ACKNOWLEDGEMENT

In the name of Allah, the Most Gracious, Most Merciful. Praise be to Allah S.W.T, Peace and blessings of Allah be upon His Messenger, Muhammad S.A.W, and all his family and companions.

I would like to express my gratitude to Prof. Dr. Ahmad Termizi Ramli, Dr. David Andrew Bradley and Prof. Dr. Husin Wagiran for their supervision, support, and encouragement throughout the course of these studies. I am sincerely grateful to the government of Malaysia and to Universiti Teknologi Malaysia for a funded PhD scholarship. I am also indebted to the Academy of Sciences Malaysia, Ministry of Science, Technology and Innovation of Malaysia and Ministry of Higher Education of Malaysia for providing research grants for this project. I am also grateful to the management and staff of the Surrey Ion Beam Centre for making available beamtime to carry out a large part of the studies featured herein. I am grateful to the Medical Physics Department of the Royal Surrey County Hospital for allowing access to the megavoltage X-ray machines situated at the hospital, in particular to Prof. Dr. Andrew Nisbet and Russel Thomas for helping out with irradiation studies. I would like to acknowledge the support of technical staff at the Physics Department, University of Surrey and Universiti Teknologi Malaysia and Ibnu Sina Institute, in particular, James Wallbank, John William Brown, Saiful, Nazri, Wani and Haliza for their assistance and cooperation.

I am similarly grateful to the Nuclear Agency Malaysia and the Department of Oncology and Radiotherapy, Hospital Sultan Ismail for giving an outstanding help and guidance in the early stage of this project, in particular, Dr. Zaharuddin, Mr. Hadi, Mr. Taiman, Mr. Hassan, Miss Nora and Mr. Izwan.

ABSTRACT

This work concerns the suitability of doped SiO₂ fibres as ionizing radiation dosimeters. The physical characters of the amorphous medium are discussed, as is the origin of the thermoluminescence (TL) signal and desirable characteristics of such a dosimeter. Facilities supporting characterization of the fibres are outlined, including an ion beam facility used for Particle Induced X-ray Emission and Rutherford Back Scattering analysis used to localize and determine the concentration of Ge and Al dopants. The dosimetric capabilities of Ge-, Al-, O₂-doped and pure SiO₂ optical fibres were investigated for low-energy X-rays, megavoltage photons, β -rays, accelerated electrons and accelerated protons, α -particles and fast neutrons. For Ge- and Al-doped fibres, linearity of dose responses were observed over useful radiotherapeutic dose range for 6 MV photons and 6 to 12 MeV electrons. TLD-100 provides a TL yield about 10 times that of Ge-doped fibre and about 30 times that of Al-doped fibres. The same order of sensitivity is displayed using a β -ray source. Linear dose response was also observed for 2.5 MeV protons irradiation. For α -particles the Bragg peak was localised to 4.5 cm in air from the point of emission. Strong TL response to fast neutrons was also found for Ge-doped fibres but was negligible for Al-doped fibres. These findings are supported by Monte Carlo simulations. Z_{eff} of between 11.9-13.4 and 11.7-13.7 were found for Ge- and Al-doped fibres respectively. The minimum detectable dose for Ge-, Al-doped fibres and TLD-100 chips were observed to be in the range of 30-50 μ Gy, 800-1400 μ Gy and 3-5 μ Gy respectively, for 6 MV photons, and 6-, 9- and 12 MeV electron irradiation. The peak of the glow curve is between 210°C to 240°C; the broad glow curve is characteristic of amorphous media. With oxygen forming additional defect centres in fibres, ion-implantation was used to dope pure silica with O₂ defects, implanting to the depth of 160 nm. The results show promising sensitivity on first use, although subsequent annealing leads to the loss of practically all of the dopants.

ABSTRAK

Kajian ini berkaitan dengan kesesuaian serabut SiO_2 terdop sebagai dosimeter sinaran mengion. Ciri-ciri fizikal media amorfus dibincangkan begitu juga asal usul isyarat luminesens terma dan sifat-sifat yang diperlukan pada dosimeter berkenaan. Kemudahan yang digunakan untuk mencirikan serabut dibentangkan termasuk kemudahan alur ion yang digunakan untuk teknik Pemancaran Sinar-X Aruhan Zarah (PIXE) dan analisis Serakan Balik Rutherford (RBS) untuk menentukan kedudukan dan menentukan kepekatan dopan germanium (Ge) dan aluminium (Al). Kemampuan dosimetri serabut optik SiO_2 yang didop dengan Ge, Al dan O_2 telah diselidik terhadap sinar-X tenaga rendah, foton (Megavoltan), sinar- β , elektron dan proton yang dipecutkan, zarah- α dan neutron cepat. Bagi serabut yang didop dengan Ge dan Al, sambutan luminesens terma adalah linear dengan dos radioterapeutik untuk julat tenaga foton 6 MV dan elektron 6-12 MeV dicerap. TLD-100 menunjukkan hasil luminesens terma 10 kali daripada serabut terdop Ge dan 30 kali daripada serabut terdop Al. Tertib kepekaan yang sama ditunjukkan oleh punca sinar- β . Sambutan dos yang linear juga dicerap untuk penyinaran proton 2.5 MeV. Untuk sinar- α , didapati puncak lengkung Bragg berada pada jarak 4.5 cm di udara dari titik pemancaran. Sambutan luminesens terma yang tinggi terhadap neutron cepat diperolehi untuk serabut terdop Ge tetapi boleh diabaikan untuk serabut terdop Al. Dapatan ini disokong oleh simulasi Monte Carlo. Nilai Z_{eff} (nombor atom berkesan) adalah masing-masing dalam julat 11.9-13.4 dan 11.7-13.7 bagi serabut terdop Ge dan Al. Dos minimum yang dapat dikesan untuk penyinaran 6 MV foton, electron 6-, 9- dan 12 MeV bagi serabut terdop Ge, Al dan cip TLD-100 adalah masing-masing dalam julat 30-50 μGy , 800-1400 μGy dan 3-5 μGy . Puncak lengkung berbara berada di antara 210°C ke 240°C, iaitu lengkung berbara lebar yang menjadi ciri bagi media amorfus. Oksigen membentuk pusat kecacatan tambahan dalam serabut, oleh itu teknik hunjaman ion telah digunakan untuk mendop silika tulen dengan cacat O_2 pada kedalaman 160 nm. Hasilnya menjanjikan kepekaan yang baik untuk penggunaan kali pertama. Namun, proses sepuhlindap seterusnya telah menyingkirkan hampir keseluruhan dopan.

TABLE OF CONTENTS

CHAPTER	TITLE	PAGE
	DECLARATION	ii
	DEDICATION	iii
	ACKNOWLEDGEMENT	iv
	ABSTRACT	v
	ABSTRAK	vi
	TABLE OF CONTENTS	vii
	LIST OF TABLES	xii
	LIST OF FIGURES	xiv
	LIST OF ABBREVIATIONS	xx
	LIST OF SYMBOLS	xxi
	LIST OF APPENDICES	xxiii
1	INTRODUCTION	1
	1.1 Overview	1
	1.2 Thermoluminescence phenomena	3
	1.3 The structures of silica (amorphous SiO ₂)	5
	1.4 Thermoluminescence mechanism for SiO ₂ -based glass	8
	1.4.1 Intrinsic defects	8
	1.4.1.1 The oxygen vacancy centre	9
	1.4.1.2 The self-trapped exciton	10
	1.4.2 Extrinsic defects or impurity centres	12
	1.4.2.1 Silicon rich silica	12

1.4.2.2	Germanium impurity	13
1.4.2.3	Aluminium impurity	13
1.5	Thermoluminescence studies on optical fibres	14
1.5.1	Germanium doped optical fibre	14
1.5.2	Erbium doped optical fibre	15
1.5.3	Neodymium doped optical fibre	15
1.6	Statements of hypotheses	16
1.7	Objectives of the study	16
1.8	Scope of the thesis	17
2	LITERATURE REVIEW	19
2.1	Theoretical models of thermoluminescence	19
2.1.1	First order kinetics	19
2.1.2	Second and general order kinetics	21
2.1.3	Adirovitch theory	23
2.2	Glow curves analysis	24
2.2.1	Initial rise method	25
2.2.2	Peak shape method	26
2.2.3	Method by Booth and Bohun	29
2.2.4	Method by Hoogenstraaten	30
2.2.5	Halperin and Braner's method	30
2.3	Interaction of radiation with matter	32
2.3.1	Interaction of photons	32
2.3.1.1	Photoelectric absorption	32
2.3.1.2	Compton Scattering	34
2.3.1.3	Pair Production	35
2.3.2	Interaction of fast electrons	35
2.3.3	Interaction of heavy charged particles	36
2.3.4	Interaction of neutrons	38
2.4	Principle of TLD	39

2.5	Characteristics of TLD	42
2.5.1	Glow curve	44
2.5.2	Sensitivity	45
2.5.3	Annealing	46
2.5.4	Dose response	47
2.5.5	Reproducibility and stability	48
2.5.5.1	Thermal fading	49
2.5.5.2	Optical bleaching	50
2.5.6	Energy response	50
2.5.7	Minimum detectable dose	53
2.5.8	Dose rate	54
2.5.9	Accuracy and precision	54
2.6	Modified Chemical Vapour Deposition (MCVD)	55
2.7	Ion Beam Analysis and Ion Implantation Technique	57
3	METHODOLOGY	62
3.1	Thermoluminescence Measurement	62
3.2	TLD reader system	63
3.2.1	Heating system	65
3.2.1.1	Preheat phase	66
3.2.1.2	Read Phase	66
3.2.1.3	Anneal Phase	67
3.2.2	Background Noise	67
3.2.2.1	Dark current	67
3.2.2.2	Thermal radiation	68
3.2.2.3	Visible radiation	68
3.2.2.4	Spurious luminescence	68
3.2.3	PMT Noise	69
3.2.4	Test Light	69
3.3	TL measurement cycle	69
3.3.1	Sample preparation	69

3.3.2	Storage and handling	72
3.3.3	Annealing	72
3.3.4	Irradiation	74
3.3.4.1	X-ray photons	76
3.3.4.2	Photon and electron irradiations	77
3.3.4.3	Proton irradiation	80
3.3.4.4	Alpha irradiation	81
3.3.4.5	^{90}Sr / ^{90}Y beta particle source irradiator	83
3.3.4.6	Neutron irradiation	85
3.4	Ion Beam based Elemental Mapping	86
3.5	Ion Implantation Technique	87
3.6	SEM (Scanning Electron Microscope) and EDXRS (Energy Dispersive X-ray Spectroscopy) analysis	89
4	TL MEASUREMENTS	91
4.1	Introduction	91
4.2	TL: Ge-doped SiO_2 optical fibre (Telekom Malaysia Research & Development Sdn. Bhd.) and TLD-700 measurements	92
4.2.1	Elemental mappings	92
4.2.2	Dependence of TL response on the mass of optical fibre	95
4.2.3	Dose response	96
4.2.3.1	Proton irradiation	96
4.2.3.2	Alpha particle irradiation	98
4.2.3.3	X-ray photons	99
4.2.4	TL glow curve	100
4.2.5	Fading	102
4.3	TL: Ge-doped, Al-doped, O_2 -doped, pure SiO_2 optical fibre (INOCORP, Canada) and TLD-100 chips and rods measurements	105
4.3.1	Brief introduction of TL measurements	105
4.3.2	Elemental mappings	106

4.3.3	Dose response	109
4.3.3.1	Proton irradiation	109
4.3.3.2	Alpha particle irradiation	115
4.3.3.3	Photon and electron irradiations	120
4.3.3.4	Beta particle irradiation	134
4.3.3.5	Neutron irradiation	136
4.3.4	SEM and EDXRS analysis	140
4.3.4.1	Effective atomic number, Z_{eff}	141
4.3.5	TL glow curve	142
4.3.6	Fading (photon and electron cases)	144
4.3.7	Reproducibility	149
4.3.8	Residual signal	151
4.3.9	Sensitivity and the minimum detectable dose	152
5	CONCLUSION	155
5.1	Summary of findings	155
5.2	Recommendations and future research	159
	REFERENCES	160
	Appendices A-D	174

LIST OF TABLES

TABLE NO.	TITLE	PAGE
1.1	Values for activation energy, E, and frequency factors, s, for Ge doped optical fibres obtained by Abdulla <i>et al.</i> (2001).	14
4.1	Ge-doped optical fibre proton response.	110
4.2	Al-doped optical fibre proton response.	112
4.3	O ₂ -doped optical fibre proton response from analysis of the RBS spectrum.	113
4.4	Ge-doped optical fibre proton response from analysis of the RBS spectrum.	114
4.5	TL yield for 6 MV photon irradiation for the various TL materials and doses investigated.	121
4.6	TL yield for 6 MV photon irradiation for the various optical fibres and doses investigated.	122
4.7	TL yield for 6-, 9- and 12 MeV electron irradiations for the Al-doped fibres doses investigated.	125
4.8	TL yield for 6, 9 and 12 MeV electrons irradiation for Ge-doped optical fibre.	126
4.9	TL yield for 6, 9 and 12 MeV electrons irradiation for TLD-100H chips.	127
4.10	TL sensitivity (TL yield.mg ⁻¹ .Gy ⁻¹) for Ge-, O ₂ -, Al-doped and pure silica fibres.	131
4.11	TL yield for Ge- and Al-doped optical fibres subjected to β -particle irradiation as provided by a ⁹⁰ Sr / ⁹⁰ Y source.	135
4.12	Fading of TL signal for Al- doped optical fibre for 6 MV photon irradiation. Example doses of 1 and 4 Gy were used.	145
4.13	TL fading for Ge- doped optical fibre for 6 MV photon irradiation. Example doses of 1 and 4 Gy were used.	146
4.14	TL fading for Al-doped optical fibre 9 MeV electron irradiation. Example doses of 1 and 3.5 Gy were used.	147
4.15	TL fading for Ge-doped optical fibres for 12 MeV electron irradiation. Example doses of 1 and 3.5 Gy were used.	148

4.16	Summary of percentage loss of TL signal (due to fading) over the first 24 hours post-irradiation of the optical fibres.	149
4.17	Reproducibility of Ge-doped optical fibre for 9 MeV electrons irradiation.	150
4.18	The ratio of first to second readout (TL yield) for Ge-doped optical fibres following a 1 Gy of 6 MeV electron irradiation.	151
4.19	The ratio of first to second readout (TL yield) for TLD-100 chips following a 1 Gy of 6 MeV electron irradiation.	152
4.20	The results of TL sensitivity (TL yield.mg ⁻¹ .Gy ⁻¹) for Ge- and Al-doped optical fibres with various electron energy irradiations and 6 MV photon irradiation.	153
4.21	A summary of minimum detectable dose for various TL materials.	154

LIST OF FIGURES

FIGURE NO.	TITLE	PAGE
1.1	A simplified energy level diagram for the thermoluminescence phenomena. Here, N is an electron trap, P is the hole trap, and M is the recombination centre (Yusoff, 2005).	4
1.2	SiO ₂ structural phase diagram (Bakos, 2003).	6
1.3	SiO ₄ tetrahedral coordination is the most common structural unit for SiO ₂ (Bakos, 2003).	7
1.4	Oxygen distorted states proposed by Fisher <i>et al.</i> (1990). Dashed lines represent configuration for the case of perfect crystal geometry. The symbols e and h represent localization of the electron and hole respectively, for the trapped exciton.	11
2.1	Isothermal decay curves for first-, second- and ‘general’- order as shown on It vs. $\ln t$ coordinates (Chen and McKeever, 1992).	22
2.2	The geometrical shape quantities: $\tau = T_m - T_l$, $\delta = T_2 - T_m$ and $\omega = T_2 - T_l$. (Pagonis <i>et al.</i> , 2006).	29
2.3	A schematic representation of the photoelectric absorption.	33
2.4	A schematic representation of Compton Scattering.	34
2.5	A schematic representation of pair production.	35
2.6	Response characteristics of two dosimetry systems (Podgorsak, 2005).	48
2.7	Process steps for preparing lightguides by the MCVD technique (http://www.britannica.com)	56
2.8	(a) The “Ideal Fibre” preform cross-section; (b) Cross-section of fibre preform made by MCVD; (c) Internal structure of the neck-down region of an MCVD fibre perform (McNamara <i>et al.</i> , 2004).	57
2.9	Proton Induced X-Ray Emission (Kaabar, 2008).	58

2.10	Electronic transitions producing various X-ray lines (Kaabar, 2008).	59
2.11	An example of typical PIXE spectrum of a femoral head sample irradiated by 2.5 MeV proton beam (Kaabar, 2008).	60
3.1	The Solaro TLD reader system (Vinten, Reading, U.K) situated in the Physics Department of the University of Surrey (with permission).	65
3.2	Optical fibre stripper (Miller, USA) used to remove the outer polymer layer of the optical fibres.	71
3.3	The progressive steps carried out in cutting the optical fibre using an optical fibre cleaver (Fujikura, Japan); [1] Optical fibre cleaver opened to receive the optical fibre; [2] Firm fixation of the fibre by means of the arrowed bridge; [3] Cutting arm brought down to cut fibre into lengths of approximately 0.5 cm each.	71
3.4	TL materials can be transferred to and from the TLD reader planchet with manual or vacuum tweezers.	72
3.5	The equipment used for containment of the TL materials for annealing.	73
3.6	A furnace (Carbolite, U.K) was used to anneal TL materials.	74
3.7	Irradiation of Ge-doped optical fibre using an X-ray beam generated at 49.8 kVp and 986 μ A.	77
3.8	The Varian Clinac 2100C linear accelerator machine situated at the Royal Surrey County Hospital (RSCH). The dose rate of 200 MU/min was used for all the photon and electron irradiations.	78
3.9	The standard size of the solid water phantom is 30 x 30 cm^2 and is available in accurate sized thicknesses, from 0.2 cm to 2 cm.	79
3.10	[1] The High Voltage 2.0 MV Tandetron TM accelerator providing 2.5 MeV protons situated in the Surrey Ion Beam Centre; [2] Four rows of doped optical fibres were attached to an aluminium plate sample holder; [3] Magnified image of fibres on the beam line as viewed using a microscope and monitor display, showing three of the fibres end on; [4] Samples of the optical fibres aligned at the sample position of the microbeam line, as viewed through one of the transparent port windows.	81

3.11	The TL materials were attached to the transparent ruler at various positions along it to allow irradiation at a range of distances.	82
3.12	The alpha exposure was performed for 24 hours in a bell jar to allow the air pressure to be maintained at 750 ± 10 mmHg.	83
3.13	The turntable is rotated at a constant speed, so that all the dosimeters receive the same dose when passing a fixed $^{90}\text{Sr} / ^{90}\text{Y}$ source.	84
3.14	The TL materials, which comprise Al- and Ge-doped silica fibres, were exposed in close contact at approximately 1 cm from the source surface of the $^{241}\text{AmBe}$ source.	85
3.15	A schematic diagram of Ion Implanter 1090 (Danfysik, Denmark) that was used to introduce oxygen dopants to the pure silica optical fibres by bombarding the fibre with the oxygen atoms.	88
3.16	A series of the pure silica optical fibres were aligned and sandwiched between the two aluminium plates of the sample holder.	88
3.17	The pure silica optical fibres prior to oxygen implantation. The implantation was carried out over a period of approximately 2 hours for each side of the sample.	89
3.18	(a) A sputtering machine was used for the gold coating procedure, the gold being deposited in order to allow leakage of charge build-up to minimize the electrostatic effect during the scanning process; (b) The samples were ready for scanning, scanning being performed across the surface and cross-sectional area of the optical fibre core.	90
3.19	A combined SEM and EDXRF analysis facility based on GEMINI technology, Zeiss, Germany, (Oxford Instruments Analytical, 2002).	90
4.1	Uncorrected relative distribution of elemental presence of Ge, Si and O in the core of a typical Ge-doped optical fibre, represented in grayscale. Note that the highly localized concentration of germanium in the central part of the core.	94
4.2	Individual reconstructed images of Ge, Si and O.	94

4.3	TL response as a function of the optical fibre mass. Departure from linearity at low fibre mass is almost certainly due to a poor signal-to-background ratio.	95
4.4	TL yield of proton-irradiated Ge-doped fibre, exposed for various length of times.	97
4.5	TL yield of Ge-doped fibre subjected to proton irradiation (the dose-rate was estimated to be $\sim 0.2 \text{ mGy s}^{-1}$).	97
4.6	(a) simulation obtained in SiO_2 (b) simulation obtained in LiF. The results show the change in stopping power over the final $25 \text{ }\mu\text{m}$ of path length measured in these two media.	98
4.7	TL response of Ge-doped optical fibre subjected to X-ray irradiation. Dose linearity is observed up to at least 10 Gy.	100
4.8	Glow curves of TLD-700 (LiF:Mg,Ti) and Ge-doped optical fibre for 2 Gy X-ray irradiation.	101
4.9	Glow curves of TLD-700 (LiF:Mg,Ti) and Ge-doped optical fibre for 10 Gy X-ray irradiation.	103
4.10	Fading of signal for Ge-doped optical fibres, irradiated to an X-ray dose of 2 Gy. After six days, the Ge-doped optical fibre showed a maximum fading of 26.2 %.	103
4.11	Fading of signal for TLD-700, irradiated to an X-ray dose of 2 Gy. After six days, TLD-700 (LiF:Mg,Ti) showed a maximum fading of 75.9%.	104
4.12	Fading of signal for Ge-doped optical fibres, irradiated to an X-ray dose of 10 Gy. After six days, the Ge-doped optical fibre showed a maximum fading of 19.7 %.	104
4.13	Fading of signal for TLD-700, irradiated to an X-ray dose of 10 Gy. After six days, TLD-700 (LiF:Mg,Ti) showed a maximum fading of 36.1 %.	105
4.14	(a) During proton irradiations for PIXE and RBS analysis, the optical fibres were sandwiched in a parallel orientation and held between two custom made copper blocks. (b) The pointed markers were used for easy viewing and to make sure the irradiation was performed on the correct fibres.	107
4.15	$300 \text{ }\mu\text{m}$ maps across the cross section of a SiO_2 optical fibre showing the presence of Si in the left hand figure and the Al dopant in the right hand figure (obtained using K_{α_1} mapping).	108

4.16	Ge-doped optical fibre response to 2.5 MeV proton irradiation.	110
4.17	PIXE and RBS map for Ge-doped SiO ₂ optical fibre.	111
4.18	Al-doped optical fibre for 2.5 MeV proton irradiation.	112
4.19	O ₂ -doped optical fibre of 2.5 MeV proton irradiation.	113
4.20	Ge-doped optical fibre of 2.5 MeV proton irradiation.	114
4.21	The relative TL yield at the position of the Bragg peak is: Ge-doped fibre TL yield ~ 3x that of Al-doped fibres.	116
4.22	Bragg peak obtained at a depth of 4.5 cm path length for TLD-100 rods.	117
4.23	Glow curve (in blue) for the Ge-doped optical fibre material following alpha particle irradiation. The time temperature profile (TTP) is shown in red.	118
4.24	Glow curve for TLD-100 rods following alpha particle irradiation.	118
4.25	TL dose response for 6 MV photon irradiation for the various TL material. The curve provided for TLD-100 chips and rods is clearly showing agreement between the two types of TLD-100 media.	121
4.26	TL dose response for 6 MV photon irradiation for Al-doped fibre and pure silica.	122
4.27	TL dose response for 6 MV photon irradiation for Ge-doped fibres.	123
4.28	TL yield for 6, 9 and 12 MeV electrons irradiation for the Al-doped fibres doses investigated. The slope was found to be $1.13 \times 10^5 \text{ mg}^{-1} \text{ Gy}^{-1}$.	125
4.29	TL yield for Ge-doped optical fibre for 6-, 9- and 12 MeV electrons and 6 MV photons irradiation. The line represents a least squares fit to the data.	126
4.30	TL yield for 6, 9 and 12 MeV electrons irradiation for TLD-100H chip. The line represents a least squares fit to the data.	127
4.31	The TL response of silica based optical fibres obtained from 6 MV photons irradiation.	128
4.32	The TL response of silica based optical fibres obtained from 6 MeV electrons irradiation.	129
4.33	The TL response of silica based optical fibres obtained from 9 MeV electrons irradiation.	130

4.34	The TL response of silica based optical fibres obtained from 12 MeV electrons irradiation.	131
4.35	The TL response of O ₂ -doped optical fibres from 6 MV, 6-, 9- and 12 MeV photon and electron irradiations obtained before annealing and after the annealing process.	133
4.36	The TL response of Ge- and Al-doped optical fibres subjected to β -particle irradiation provided by a ⁹⁰ Sr / ⁹⁰ Y source.	134
4.37	TL intensity of Ge- and Al-doped optical fibres irradiated to fast neutrons. The results were compared with MCNP5 simulations. The line represents a least squares fit to the data.	137
4.38	Logarithmic plot of the TL response to fast neutrons of Ge- and Al-doped optical fibres using the data previously shown in Figure 4.37.	138
4.39	The curve of the cross section in the fast neutron (> 1 MeV) region: the blue curve is for ⁷⁰ Ge, the green curve is for ²⁸ Si and the red curve is for ²⁷ Al.	140
4.40	A typical optical fibre glow curve displaying the characteristic a single broad peak of an amorphous medium.	143
4.41	TL fading for Al-doped optical fibres for 6 MV photons irradiation.	145
4.42	TL fading for Ge-doped optical fibre for 6 MV photons irradiation.	146
4.43	TL fading for Al-doped optical fibres for 9 MeV electrons irradiation.	147
4.44	TL fading for Ge-doped optical fibres for 12 MeV electrons irradiation.	148
4.45	Reproducibility studies of Ge-doped fibres at 9 MeV electrons irradiation. Note that the second exposure (red points) was obtained after performing full annealing procedures and repeating the same parameters for the irradiation.	150
4.46	The sensitivity obtained from the TL materials subjected to 9 MeV electrons irradiation.	153

LIST OF ABBREVIATIONS

NAME	DEFINITION
TLD	Thermoluminescence dosimetry
ICRU	International Commission of Radiation Units
TL	Thermoluminescence
TLD phosphors	TLD-100 or TLD-700
STE	Self-trapped exciton
DFT	Density functional theory
ODMC	Optically detected magnetic resonance
LET	Linear energy transfer
IR	Infra-red
PMT	Photomultiplier Tube
MCVD	Modified Chemical Vapour Deposition
PTFE	Polytetrafluoroethylene
Si(Li)	Lithium drifted silicon detectors
LINAC	Linear accelerator
PIXE	Proton-induced x-ray emission
RBS	Rutherford back scattering
SEM	Scanning electron microscope
EDXRF	Energy dispersive x-ray spectroscopy
OSL	Optically stimulated luminescence
MCNP	Monte Carlo N-Particle

LIST OF SYMBOLS

ΔE	Energy of the photoelectron
E	Incident photon energy
E_o	Binding energy of the orbital electron
τ	Photoelectric mass attenuation coefficient
Z	Atomic number of the atom
θ	Small scattering angle
E_γ	Energy of the incident photon
$E_{\gamma'}$	Energy of the scattered photon
$m_o c^2$	Rest-mass energy of electron (0.511 MeV)
E_{max}	The maximum energy
m	The charged particle mass
S	The linear stopping power
dE	The differential energy loss
dx	The corresponding path length
m_o	The electron rest-mass
e	The electronic charge
v	Velocity
ze	Charge of the primary particle
I	The average excitation
N	The number density
c	Velocity of light
D	Absorbed dose
Gy	Gray
LiF	Lithium fluoride
$CaSO_4$	Calcium sulphate

E_t	A trap of depth
k	Boltzmann constant
T	Temperature
n	Number of electrons in a particular trap energy
B_{mean}	The mean TL background signal
σ	The standard deviation
F	TL system calibration factor
D_o	Threshold dose
C	Coulomb
N_2	Nitrogen gas
SiO_2	Silicon dioxide
GeO_2	Germanium dioxide
Al_2O_3	Aluminium oxide
MU	Monitor Units
Z_{eff}	The effective atomic number

LIST OF APPENDICES

APPENDIX	TITLE	PAGE
A	Calculation of neutron to photon ratio	174
B	A source code for neutron simulation using MCNP5	175
C	The whole experimental set-up with MCNP5 boundary	177
D	List of Publications	178

CHAPTER 1

INTRODUCTION

1.1 Overview

Thermoluminescence dosimetry (TLD) is generally acknowledged to be the most widely used and cost-effective technique for radiation dosimetry, being almost certainly the most popular technique for routine monitoring of occupational radiation exposure (Portal, 1981). TLD phosphors are widely applied in medicine to determine patient dose arising from diagnostic X-ray procedures and cancer radiotherapy treatments. The dose ranges of interest are approximately 0.01 - 1 mSv for personal dosimetry, 0.1 - 100 mSv for clinical X-ray diagnosis and 1 - 5 Sv for radiotherapy (ICRU, 1998). Rassiah *et al.* (2004) reported that there are currently 17 megavoltage radiotherapy centres to serve a population of 23.3 million in Malaysia. This large number of therapy centres has paved the way for medical therapy researchers to investigate issue of consistency on dose delivery to the patients. The International Commission of Radiation Units (ICRU) recommends that the accuracy of the dose delivered to the target volumes in radiotherapy should be within $\pm 5\%$ (ICRU, 1976).

TLD phosphors most typically used in medical applications are LiF:Mg,Ti and LiF:Mg,Cu,P due to their tissue equivalence characteristics. However, these well established materials have several notable drawbacks, including being hygroscopic and having relatively poor spatial resolution, ~ up to a few mm (McKeever and Moscovitch, 2003). With these restrictions in mind, novel TLD materials are

currently identified, based on doped SiO₂ optical fibres, which offer characteristics that provide good potential for broadening the applicability of TLD.

Compared with the use of TLD phosphors, the fibres not only offer the possibility of improved positional sensitivity (fibre diameters are sub-millimeter, typically $\sim 200\ \mu\text{m}$) but also, since the fibres are impervious to water (the silicates forming a glass in the fibre-preforming process), this paves the way for their use in inter-cavitary and interstitial measurements (Abdulla *et al.*, 2001b). Such capability, in conjunction with the appreciable flexibility of the fibres (accommodating relatively small radii of curvature) also makes a fibre dosimetry system suitable for studies related to intra-coronary artery brachytherapy. Application of radiation doses to artery walls to prevent re-stenosis following balloon angioplasty is a technique that has recently gained widespread attention within the radiotherapy community. The capability of fibre TL systems also promises to be of considerable interest for dosimetry in a variety of vascular procedures involving high radiation doses to the skin, such as procedures being carried out under fluoroscopic guidance. In patients with severe medical problems for whom few, or no, alternative diagnostic techniques can be envisaged, doses have been delivered to an extent resulting in severe skin necroses (Aznar *et al.*, 2002). Geise and O'Dea (1999), cite doses of several tens of Gy to the skin in several such medical investigations, also reviewing moves towards ensuring skin dose reduction in so far as this may be possible for the particular situation. At this point it is sufficient to point out that there are many interesting dosimetric applications of optical fibres that could be imagined in such situations.

For optical communication, dopants within glass fibres are used to control the refractive index of the glassy host (Bhadra *et al.*, 2005). Fortuitously, due to the presence of these same dopants, irradiated glass fibres give rise to TL to an extent well beyond that of the silica itself. Useful intensities of TL have been observed at radiation levels familiar in high dose radiation-medicine procedures. In optical fibre systems, dopants added to the core structure provide for total internal reflection, these

defects being distributed under the high temperature and rapid quenching conditions that are required for fibre drawing.

1.2 Thermoluminescence phenomena

The presence of defects is the centre of the thermoluminescence phenomena. As an example, a negative ion vacancy is a region of excess positive charge and as such may be regarded as a potential electron trap (Furetta, 2003).

In a perfect crystal, there exists a bandgap between the highest valence band and the lowest conduction band where no electron or hole allowed states are possible. Whenever the perfect crystal structure is disturbed by the presence of a defect, one or more additional energy levels are introduced into the forbidden gap. The energy level for an electron trap can be located just below the conduction band. Likewise, a hole trap can produce an energy level just above the valence band. However, unlike the perfect crystal energy bands, which extend throughout the crystal, the additional levels are localized at the crystal defect. Figure 1.1 shows a simple representational view of energy levels in a solid containing defects.

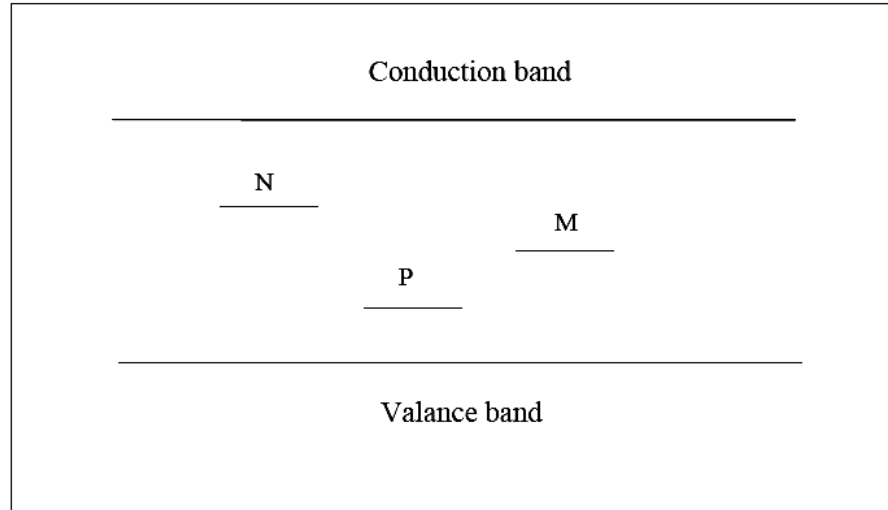


Figure 1.1: A simplified energy level diagram for the thermoluminescence phenomena. Here, N is an electron trap, P is the hole trap, and M is the recombination centre (Yusoff, 2005a).

In its ground state, the valence band is filled while the traps and the conduction band are empty. When ionizing radiation is absorbed by the material, some electrons in the valence band will be excited to the conduction band. The excited electrons are now free to move through the crystal. The presence of defects in the crystal makes it possible however, for the electrons to become trapped. Holes, which are created in the valence band during the excitation process, can also move freely in the crystal until either they are trapped in hole traps or are recombined with electrons.

The trapped charge carriers will remain in their respective traps unless sufficient energy is acquired to allow them to escape. In thermoluminescence, the two main factors that determine the extent to which the trap emptying process occurs are the depth of the trap and the local temperature around the trap. While the trap depth is determined by intrinsic properties of the defect, the temperature is an externally controllable factor (Yusoff, 2005a). If the temperature is raised, the trapped charge carriers may acquire enough energy to escape. Subsequently, the

released electrons may recombine with holes at the recombination centres with the emission of photons of commensurate energy (wavelength).

During heating, a released charge can participate in many different kinds of process. The three main kinds of processes of importance to the thermoluminescence phenomena are retrapping of charge carriers at a defect, radiationless recombination, and luminescent recombination. Only the luminescent recombination process produces a signal which is useful for thermoluminescence production (Yusoff, 2005a). Further explanation related to TL phenomena will be discussed in section 2.4.

1.3 The structures of silica (amorphous SiO₂)

The structure of silica was reported by Bakos (2003). Silica is known to be an amorphous (or glassy) material. X-ray diffraction indicates that the structural order present in crystalline forms is preserved in such glassy media over the short and intermediate range scales. The atomic coordination and the first and second neighbour distances are very similar in the amorphous and crystalline forms indicating that the basic building blocks of the two solid states of SiO₂ are similar. The structural phase diagram of crystalline SiO₂ is shown in Figure 1.2. The most common structures of SiO₂ at low pressure are α -quartz, β -quartz, and tridymite.

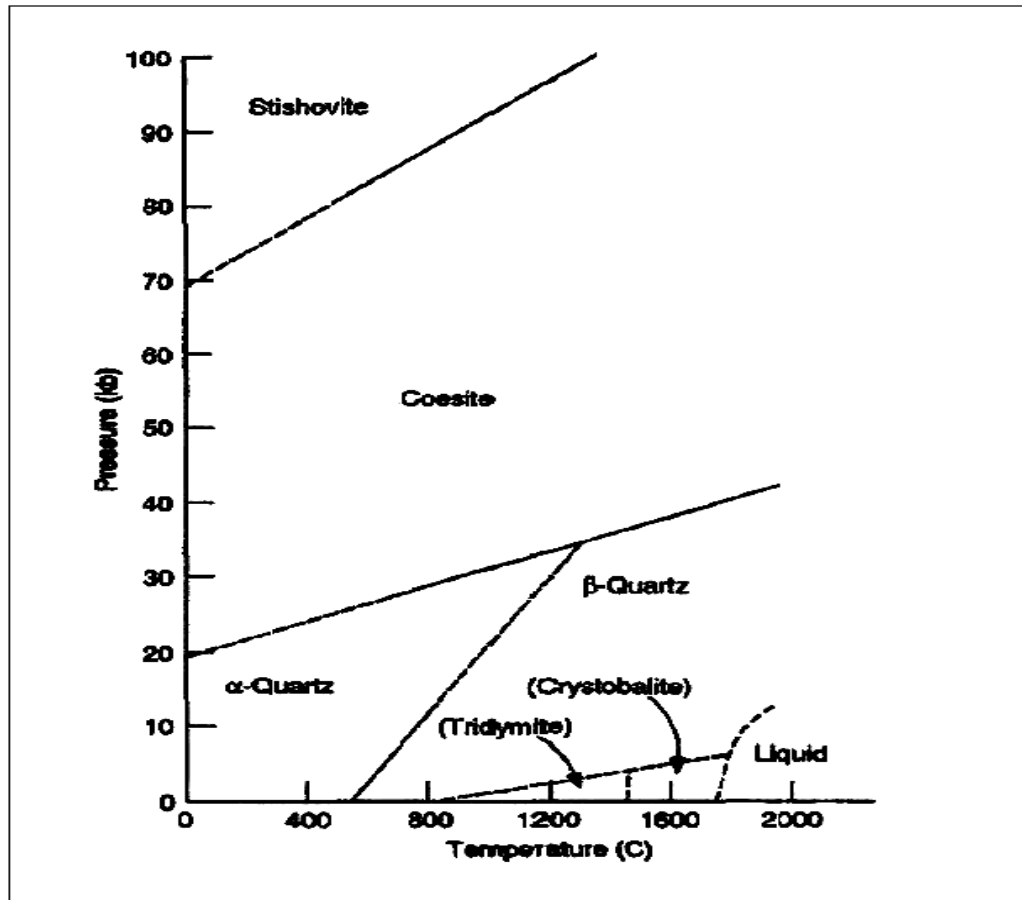


Figure 1.2: SiO₂ structural phase diagram (Bakos, 2003).

The basic bonding unit of all SiO₂ crystalline structures, except for stishovite, is a tetrahedron as shown in Figure 1.3. Each silicon atom is bonded to four oxygen atoms, with the bond lengths ranging from 1.52Å to 1.69Å. The O-Si-O bond angle is 109.18°. Each of the oxygen atoms bonds to two silicon atoms with the Si-O-Si bond angle ranging from 120° to 180°, depending on the structure. The high temperature low pressure cristobalite and tridymite possess the largest bond angles. The large bond angles reflect in the density of the material, with the larger bond angle producing less packed SiO₂ material.

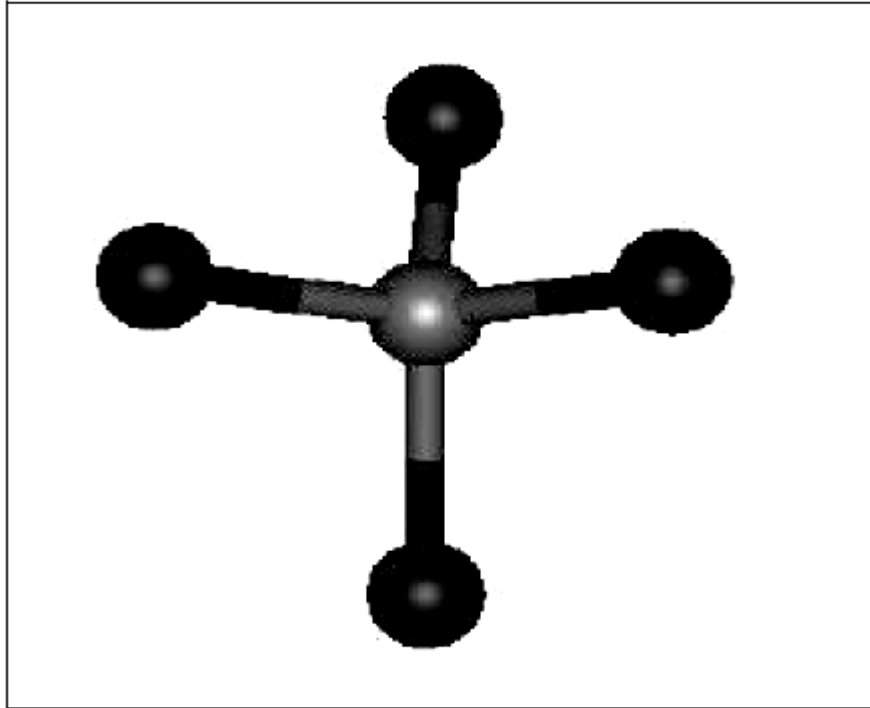


Figure 1.3: SiO_4 tetrahedral coordination is the most common structural unit for SiO_2 (Bakos, 2003).

Although the phase diagram in Figure 1.2 was derived from the case of crystalline SiO_2 , it can also be used to determine which structure might be present in an amorphous sample, in the form of micro crystallites. Since silica glass is a result of fast cooling of heated SiO_2 , the material is not allowed to relax to the low temperature structure. The most probable form of SiO_2 micro crystallite in silica glass produced at ambient pressure is tridymite, being stable up to 1470°C .

Two models exist for the structure of amorphous silica, namely, the continuous random network model and the microcrystalline model, both of which are consistent with experimental data. In the continuous random network model, the silica glass is modelled to be constructed from SiO_2 tetrahedrons with each of the oxygen atoms shared by two tetrahedrons. The only difference to the crystalline forms is the bond angle, which is allowed to vary from one tetrahedron corner to another. Therefore, the structure is a random network of tetrahedrons. In the

microcrystalline model, the silica is constructed from micro-crystallites of different structures, as in Figure 1.2 or from the sub units of the structures. By doing this, the distribution of bond angles falls within the types of structure included in the model. Within the limit of small crystallites, the two models converge (Karmakar, 2005).

1.4 Thermoluminescence mechanism for SiO₂-based glass

In this section, is a review of existing research into possible mechanisms for the luminescence phenomena in silica glass. Although almost all of this research concerns investigation of the photoluminescence phenomena in crystalline silica, the defects studied can also be considered to provide a link to the thermoluminescence in silica glass. While there are many possible defects in silica, discussion will only be made of those defects that have been studied in some detail, generally being those which have a greater probability of causing significant thermoluminescence. The defect modes can be divided into two major categories, according to whether one is dealing with intrinsic or extrinsic defects.

1.4.1 Intrinsic defects

It is meaningless to define defects in silica in the same way that they would be for a crystalline material, i.e. any disruption in the repeated structure is considered a defect, since amorphous silica does not enjoy long range order. Defects in silica are therefore defined as the disruption in the short or mid range order, in this case the disruption occurring in the normal SiO₂ tetrahedron coordination and the normal two fold coordination of the oxygen atoms. Therefore, the absence of oxygen atoms in the tetrahedrons are oxygen vacancy defects while the absence of silicon atoms are silicon vacancy defects.

One common type of defect in silica is the broken or dangling bond. This type of defect leaves atoms with dangling orbitals that are populated by unpaired electrons. Thus, this type of defect is paramagnetic and therefore is detectable using the electron spin resonance (ESR) technique. The main defects that fall into this category are the non-bridging-oxygen (NBO) centre ($\text{O}_3\equiv\text{Si}-\text{O}\cdot$), the proxy radical, and variations of E' centre, namely the oxygen vacancy.

Diamagnetic defects (an example of which is given below) are not detectable by ESR. In this case, the defects are studied by mapping out their energy levels using absorption, luminescence, or photoionization spectroscopy. One important diamagnetic defect in silica is the neutral oxygen vacancy where the Si-Si bond is formed, being usually a precursor to one of the E' centre type of defect.

One important feature of the intrinsic defect is that the number of these is temperature dependent. For silica, the two main defects within this category are the oxygen vacancy centre and the self-trapped exciton, a defect resulting from the interaction between an excited electron with the corresponding hole left in the valence band, to be explained further in section 1.4.1.2.

1.4.1.1 The oxygen vacancy centre

Perfect crystalline silica will comprise of single silicon atoms surrounded by four oxygen atoms. Each of these oxygen atoms forms a bridge between two silicon atoms. In this way charge neutrality is conserved within the crystal. If one oxygen atom is missing, the local charge becomes positive. As such, it becomes a possible electron trap. In silica, this trap is called the E' centre, being analogous to the well known F centre in alkali halides. Variations of the E' centre, i.e. an oxygen vacancy results in dangling silicon sp^3 bonds as summarized by Warren *et al.* (1992).

An analysis of the E' centre by Silsbee (1961) has determined the existence of an unpaired spin localized at the sp^3 orbital of the silicon atom with orbital orientation towards the oxygen vacancy position. According to Fowler and Edwards (1997), if the two adjacent silicon atoms relax asymmetrically, this being the most likely occurrence in glass due to its inherent asymmetry, then one electron can stabilize itself on one of the silicon atoms. Electron spin resonance (ESR) studies in silica glass by Griscom (1979) have revealed that the same E' structure exists in silica glass.

With an oxygen vacancy, it is also possible for the atom to rearrange itself to form a Si-Si bond, which also maintains local charge neutrality. This happens when both silicon atoms adjacent to the oxygen vacancy relax towards each other. Tsai *et al.* (1988) have suggested that this arrangement is a result of non-radiative decay of an exciton (see below for an explanation of the exciton), the Si-Si centre forming a hole trap. They have estimated that the exciton binding energy in SiO_2 is about 1.3 eV. The E' centre can also transform into a Si-Si centre at high annealing temperature. At even higher annealing temperature, the Si-Si centres tend to transform themselves into excess silicon atoms in SiO_2 (Rebohle *et al.*, 1998).

1.4.1.2 The self-trapped exciton

When an electron is excited in a lattice it will leave a hole in the valence band. This electron will experience a coulombic interaction with the hole, screened by ions and other electrons. This electron-hole pair, termed an exciton, can propagate through the crystal. In SiO_2 , the electron-hole pair is strongly bound due to the low dielectric constant of the base compound. The presence of the self-trapped exciton (STE) in SiO_2 leads to an energy level inside of the normal bandgap.

The existence of a photoluminescence band at 440 nm in SiO_2 supports the suggestion that excitons are trapped in the SiO_2 matrix, a phenomenon which will not happen in an ideal crystal. It is now accepted that the mechanism for STE in silica is the motion of oxygen atoms in the crystal. The motion, first proposed by Fisher *et al.* (1990), is an oxygen atom rotation about another Si-O bond of a neighbouring silicon atom (Figure 1.4). This motion causes a lattice distortion that significantly changes the local energy level in the crystal.

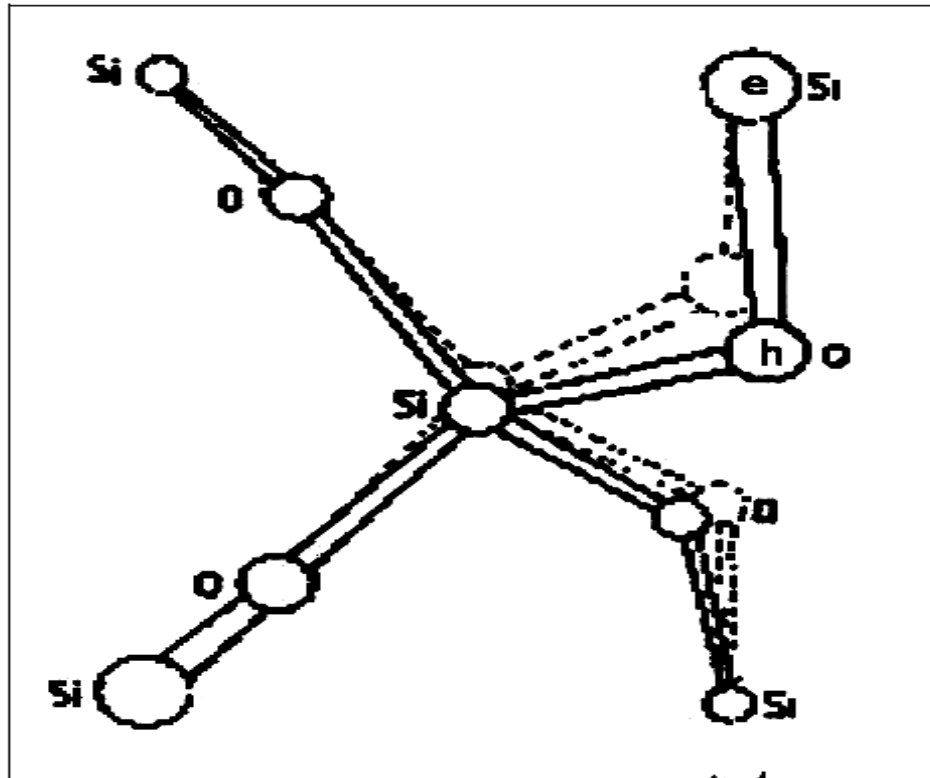


Figure 1.4: Oxygen distorted states proposed by Fisher *et al.* (1990). Dashed lines represent configuration for the case of perfect crystal geometry. The symbols e and h represent localization of the electron and hole respectively, for the trapped exciton.

A Hartree-Fock calculation on this oxygen distorted state, using the model depicted in Figure 1.4, confirmed the view that oxygen motion is the mechanism responsible for exciton trapping (Bakos, 2003). A later, more rigorous calculation using density functional theory (DFT) shows that the excited electron is localized on the antibonding molecular orbital of a silicon atom. Conversely, the hole is localized

on the molecular orbital of the three oxygen atoms. In addition to the oxygen distorted state at 2.8 eV, a silicon distorted state at 0.23 eV higher has also been found by Song *et al.* (2000).

1.4.2 Extrinsic defects or impurity centres

Analysis of luminescence when impurities are introduced into the SiO₂ substrate involves a model in which the impurity centre becomes either substitutional atoms, interstitial atoms, an impurity-intrinsic complex, or an impurity-impurity complex inside the substrate. Apart from the possibility of introducing a new luminescence band, impurity atoms might also change the number of electron or hole traps. In the following, a brief discussion is provided of a number of elemental impurity atoms, some of which have been used in commercially available telecommunication optical fibres (providing favourable optical refractive indices for total internal-reflection). Present interest is of course the thermoluminescence produced by such dopants.

1.4.2.1 Silicon rich silica

The silicon rich silica contains more oxygen defect centres than in pure silica. Accordingly, although enjoying the same spectral energy distribution, one expects more intense luminescence to result from the rich silicon silica as compared to pure silica.

1.4.2.2 Germanium impurity

Germanium atoms in SiO_2 will directly substitute for silicon atoms in the crystal. Spin resonance studies have shown that the GeO_4 unit cell and SiO_4 unit cell are similar, before and after trapping of an electron. The difference in the ionic potential of Si^{2+} and Ge^{2+} are too small to provide any impurity localized states, as reported by Hagon *et al.* (1985). However, Ge in SiO_2 is known to be a deep electron trap. An optically detected magnetic resonance (ODMC) study by Hayes and Jenkin (1988) has shown that Ge doped silica exhibits similar exciton occurrence to that existing in pure silica.

1.4.2.3 Aluminium impurity

Aluminium doped silica yields a luminescence spectra that shows the existence of an E' centre type defect (Trukhin *et al.*, 2004). In this particular case, the aluminium atom in SiO_2 is surrounded by three oxygen atoms, $\text{AlO}_{3/2}$. This arrangement is diamagnetic and also electrically neutral. At temperatures greater than 260K, the oxygen vacancy traps electrons, and the local charge around aluminium becomes negative, i.e. $\text{AlO}_{3/2}^-$.

An aluminium impurity in SiO_2 can also become a hole trap. Some aluminium atoms in silica are four-fold oxygen coordinated. For this type of coordination, the local charge is negative, i.e., $\text{AlO}_{4/2}^-$. Near room temperature and above, $\text{AlO}_{4/2}^-$ is not compensated and therefore it can trap a hole. At ground state, the trapped hole is localized on an oxygen long bond to aluminium. For excited states, the hole is localized on the short oxygen bond to aluminium (Nuttal and Weil, (1981a) and Nuttal and Weil, (1981b)). The same hole trap centre also exists in Ge doped SiO_2 , occurring when a Ge atom traps an electron to become Ge^{3+} . However, this centre is not deep enough to survive at room temperature (Hayes and Jenkin, 1988).

1.5 Thermoluminescence studies on optical fibres

Early studies involving photon irradiation effects of silica based optical fibres were carried out by, among others, Friebele (1979), Friebele *et al.* (1980, 1984), Kirsh *et al.* (1989), Ellis *et al.* (1989), Khanlary *et al.* (1993) and Abdulla *et al.* (2001a). These investigations have determined that the TL performance of an irradiated optical fibre is influenced by the type of fibre and by the radiation parameters. Presented herein are a few of the studies that suggest development of TL dosimeter materials from doped silica fibres.

1.5.1 Germanium doped optical fibre

Abdulla *et al.* (2001b) has carried out a TL study on commercially available Ge-doped silica based optical fibres. The fibre was prepared in the form of 1 cm length rods (~ 0.3 mg each), and the samples were irradiated using a gamma source. The radiation dose range investigated was 1-1230 Gy. The TL glow curve parameters are summarized in Table 1.1.

Table 1.1: Values for activation energy E , and frequency factors s , for Ge-doped optical fibres obtained by Abdulla *et al.* (2001b).

Peak	Temperature (°C)	E (eV)	s (s ⁻¹)
1	100	0.80	1.20×10^{12}
2	140	0.99	2.30×10^{13}
3	325	1.42	1.22×10^{13}
4	399	1.56	5.48×10^{12}

Good reproducibility of TL readout through five repeat cycle of annealing-irradiation-readout was found (correlation coefficient = 0.95). In addition, the dose response for the fibre was found to be linear from 1 to 120 Gy. The TL signal from Ge doped fibre has a fast fading characteristic of about 2% within 6 hours

and a slow fading of 7% within 30 days. It was claimed that the lower detectable limit of radiation dose for this type of optical fibre is 0.02 Gy (Abdulla, 2003).

1.5.2 Erbium doped optical fibre

Work on this dopant also has been carried out by Abdulla *et al.* (2001c) using commercially available Er doped silica based optical fibre. The main feature of the TL glow curve is that it produces a single glow peak at about 150°C. The activation energy (E) and the frequency factor (s) were calculated using four methods: the peak shape method, Grossweriner, Lushchik and the initial rise method. The first three methods gives value of 0.3 eV to 0.4 eV and the last method gives a value of 0.67 eV. The dose range investigated was 2-400 Gy, the dose response being found to be linear up to about 250 Gy. Significant fading of the TL signal from Er doped fibre has been found, nearly 30% of TL signal being lost after the first 24 hours. After 20 days of storage at room temperature, a total loss of 58.6% of TL signal was reported.

1.5.3 Neodymium doped optical fibre

Safitri *et al.* (2006) has observed that the Nd-doped silica fibres provide high dose response subjected to photon and electron irradiations. The Nd-doped fibres within the energy of 0.06 - 20 MeV has an effective atomic number of about 13.32 – 21.41. The TL glow curve shows a broad peak characteristic at ~ 192 °C. A complete annealing process was found at 400 °C for one hour. The TL fading up to 12.5% over 30 days was recorded following 202.2 mGy X-rays irradiation.

1.6 Statements of hypotheses

The hypotheses used are as follows:

1. The optical fibres investigated are typical single-mode fibres. The irradiations on the core of the optical fibre have been conducted at various doses for different types of ionizing radiation sources (photons, electrons and protons which are accelerated and neutrons, alpha and beta particles).
2. It is known that the pure silica will give rise to a degree of thermoluminescence (TL) following irradiation by ionizing radiation, the TL signal is considerably enhanced by the presence of certain dopants.
3. The exact amount of dopant added to these fibres is not specified by the manufacturers. The dopant acts as the defect centres that provide the TL signal. Of possible concern is the non-uniformities in the distribution of added dopants and impurity concentration in the core of the optical fibres which may contribute to variation in TL yield.

1.7 Objectives of the study

The objectives of this study are:

1. To provide fundamental dosimetric properties of doped SiO₂ optical fibres i.e. effective atomic number, linearity and sensitivity with respect to dose response, TL glow curve, fading, residual studies and reproducibility.
2. To understand the TL dependency with dopant and dopant concentration, so that the sensitivity of the measurement is acceptably high and the dose response is linear within the dose range of interest for medical applications.

1.8 Scope of the thesis

In regard to this doctoral thesis, an important characteristic of dosimeters such as fading, TL glow curve, residual signal studies, reproducibility and sensitivity characteristic of these fibres will be explored, as well as their dose dependency using photon, neutrons and charged particle ionizing radiations.

The methods of analyzing the TL glow curves will be described theoretically in Chapter 2. No glow curve analysis will be conducted to obtain the values of kinetics parameters (activation energy E and frequency factor s). The study on TL dosimetric properties such as the annealing condition, glow curves parameters, energy dependence, relative energy response, dose rate effect, heating rate effect and optical bleaching have also been omitted. These have been studied in detail by Abdulla, Y.A (2003) and Safitri *et al.* (2006). However, their studies only used accelerated photons and electrons from linear accelerator (linac). It is important to try different approach with the aim to understand the dependency of TL signal on variety of dopants, dopant concentrations and different types of radiation sources. This study may provide a basis for exploiting TL phenomena for various dosimetric situations.

Although producing optical fibre dosimeters appears to be of great interest, the scientific problem involved in producing such a dosimeter lies within the development of suitable silica based material that is sufficiently sensitive to radiation dose. In the studies presented herein, results from research on variously doped SiO₂ (Ge-, Al-, O₂-doped and pure silica optical fibres) will be compared against commercially available TLD phosphors (TLD-100 and TLD-700). Findings from these studies may pave the way to conduct more comprehensive investigation of TL from tailor-made doped SiO₂ optical fibres.

The present chapter, has provided introduction to the problems associated with TL and a review of the existing literature regarding the subject. Chapter 2 addresses the TL models, radiation interactions, principle of TLD and their important characteristics as a radiation dosimeter and brief introduction to the technique related in this study. Chapter 3 describes the methodology and equipment used. In chapter 4, a range of thermoluminescence studies and the results obtained are presented and discussed in detail. Chapter 5 summarizes the findings of this investigation, and provides an outlook for future study in this area.

REFERENCES

- Abdul Aziz Mat Hassan (Dr.) (2008). Telekom Malaysia Research & Development Sdn. Bhd. (TMR&D), personal communication.
- Abdulla, Y.A., Amin, Y.M. and Bradley, D.A. (2001a). Dosimetric characterisation or Erbium-doped optical fibre as thermoluminescence material. not published.
- Abdulla, Y.A., Amin, Y.M. and Bradley, D.A. (2001b). The thermoluminescence response of Ge-doped optical fibre subjected to photon irradiation. *Radiation Physics and Chemistry*, 61, 409–410.
- Abdulla, Y.A., Amin, Y.M and Bradley, D.A (2001c). The effect of dose and annealing on TL sensitivity of germanium and erbium doped optical fibres. *Jurnal Fizik Malaysia*, Vol. 22, No. 3 & 4, 49-53.
- Abdulla, Y.A (2003). The thermoluminescence response of Ge-doped and Er-doped optical fibres in radiation therapy. University of Malaya : PhD Thesis.
- Adirovitch (1956). La formule de Becqueral et la loi elementraire du delive de la luminescence des phosphores cristallins. *J.Phys. Rad.* Vol. 17, 705.
- Attix, F.H. (1986). Introduction to radiological physics and radiation dosimetry. New York : John Wiley & Sons.

- Aznar, M., Polf, J., Akselrod, M., Andersen, C., Back, S., Boetter-Jensen, L., Mattsson, S., McKeever, S and Medin J. (2002). Real-time optical fibre dosimetry in radiotherapy. <http://www.aapm.org/meetings/02AM/pdf/7626-20413.pdf>.
- Bakos, T. (2003). *Defects in Amorphous SiO₂: Reactions, Dynamics and Optical Properties*. Vanderbilt University : PhD Thesis.
- Balarin, M. (1975). *Phys.Stat. Sol.*, vol. 31, K 111.
- Basun, S., Imbusch, G.F., Jia, D.D and Yen, W.M. (2003). The analysis of thermoluminescence glow curves. *Journal of Luminescence*, 104, 283-294.
- Becker, K. & others (1973). *Solid State Dosimetry*. Ohio : CRC Press Inc.
- Bhadra, S.K., Paul, M.C., Bandyopadhyay, S., Pal, M., Gangopadhyay, T., Sen, R., Dasgupta, K. and Maiti, H.S. (2005). Optical fibre: Science, technology and evolution. *Science and culture*, 71, 116-130.
- Bradley, D.A., Hugtenburg, R.P., Hashim, S., Okoya O.O., Yusoff, A.L., Hassan, A.A.M., Ramli, A.T. and Wagiran, H. (2007). The Development of Doped Radiosensitive Glass. The 2nd International Conference on Solid State Science and Technology 2006; ICSSST 2006. *AIP Conference Proceedings*, Volume 909, 9-18.
- Brichard, B., Borgermans, P., Fernandez, A., Lammens, K. and Decreton, M. (2000). Radiation effects in silica fibre expose to intense mixed neutron-gamma radiation field.
http://www.sckcen.be/sckcen_en/people/affernandez/pdf/BB_TNS01.pdf.

- Briesmeister, J.F. (2003). *MCNP : A General Monte Carlo N-Particle Transport Code*, Version 5, Los Alamos National Laboratory.
- Bushberg, J.T. (2002). *The Essential Physics of Medical Physics*. 2nd edition. USA : Lippincott Williams & Wilkins.
- Chen, R. and Haber (1968). *J. Electrochem. Sec.* vol. 116, 1245.
- Chen, R. and Kirsh, Y. (1981). *Analysis of thermally Stimulated Processes*. Oxford: Pergamon Press.
- Chen, R. and McKeever, S.W.S. (1992). *Theory of Thermoluminescence and Related Phenomena*. New York : World Scientific Publisher.
- Crowther, J.A. (1938). *Ions, electrons and ionizing radiations*. 7th edition. Cambridge: London Edward Arnold & Co.
- Crundell, M. and Proctor, K. (2003). *Medical Physics: Advanced physics readers*. London : John Murray Publishers.
- Dyson, N. (1993). *Radiation physics with applications in medicine and biology*. 2nd edition. New York : Ellis Horwood Ltd.
- Edward, M.B., Harold, D.K. and Thomas, R.M. (2002). *Chart of the Nuclides*. 16th edition, USA : Knolls Atomic Power Laboratory.
- Ellis, A.E., Moskowitz, P.D., Townsend, J.E., and Townsend, P.D. (1989). An optical fibre rereadable radiation dosimeter for use at high doses and at elevated temperature. *Journal of Physics D: Applied Physics*, 22, 1758-1762.

- Espinosa, G. (2005). Thermoluminescent response of commercial SiO₂ optical fibre to gamma-radiation. *Journal of Radioanalytical and Nuclear Chemistry*, 264, 107-111.
- Espinosa, G., Golzarri, J.I., Vazquez, C. and Fragoso, R. (2003). Measurement of nano-size etched pits in SiO₂ optical fibre conduit using AFM. *Radiat. Meas.* 36, 175-178.
- Espinosa, G., Golzarri, J.I., Bogard, J. and Garcia-Macedo, J. (2006). Commercial optical fibre as TLD material. *Radiat. Prot. Dosim.*, 18, 1-4.
- Fisher, A.J., Hayes, W. and Stoneham, A.M. (1990). Structure of the self-trapped exciton in quartz. *Physical Review Letters*, 64, 2667–2670.
- Fowler, W. and Edwards, A.H. (1997). Theory of defects and defect processes in silicon dioxide. *Journal of Non-Crystalline Solids*, 222, 33–41.
- Friebele, E.J., Griscom, D.L (1979). Color centres in glass optical waveguides. *Physical Review Letters*, 42 (20), 1346-1349.
- Friebele, E.J., Schattz, P.C. and Gingerich, M.E. (1980). Compositional effects on radiation response of Ge-doped silica core optical fibre waveguides. *Appl. Opt.*, 19, 2910–2916.
- Friebele, E.J., Askirs, C.G., Gingerich, M.E. and Long, K.J. (1984). Optical fibre waveguides in radiation environments, II. *Nuclear Instruments and Methods in Physical Research B1*, 355-368.
- Furetta, C. (2003). *Handbook of thermoluminescence*. New York : World Scientific Publisher.

- Garlick, G.F.J. and Gibson, A.F. (1948). The electron trap mechanism of luminescence in sulphide and silicate phosphors. *Proc. Phys. Soc.*, vol. 60, 574-590
- Geise, R.A. and O'Dea, T.J. (1999). Radiation dose in interventional procedures. *Appl. Rad. Isot.*, 50, 173.
- Gowda, S., Krishnaveni, S., Yashoda, T., Umesh, T.K. and Gowda, R. (2004). Photon mass attenuation coefficients, effective atomic numbers and electron densities of some thermoluminescent dosimetric compounds. *PRAMANA-Journal of Physics*, 63, 529-541.
- Greening, J.R. (1981). *Fundamentals of Radiation Dosimetry : Medical Physics Handbook 15*. Bristol : Adam Hilger Ltd.
- Grime, G.W. and Dawson, M.D. (1995). Recent developments in data acquisition and processing on the Oxford scanning proton microprobe. *Nuclear Instruments and Methods in Physics Research B.*, 104, 107-113.
- Grime, G.W. (1996). The 'Q factor' method: quantitative microPIXE analysis using RBS normalization. *Nuclear Instruments and Methods in Physics Research B.*, 109/110, 170-174.
- Gripp, S., Haesing, F.W., Bueker, H. and Schmitt, G. (1998). Clinical in-vivo dosimetry using optical fibres. *Radiation Oncology Investigations*, 6, 142-149.
- Griscom, D.L. (1979). E' center in glassy SiO₂: Microwave saturation properties and confirmation of the primary ²⁹Si hyperfine structure. *Physical Review B*, 20, 1823-1834.

- Grossweiner, L.I. (1953). A note on the Analysis of first order glow curves. *J.Appl. Phys.*, 24 (10), 1306-1307.
- Hagon, J.P., Jaros, M. and Stoneham, A.M. (1985). Electronic structure of Ge in SiO₂. *Journal of Physics C: Solid State Physics*, 18, 4957–4962.
- Halperin, A. and Braner, A.A. (1960). Evaluation of thermal activation energies from glow curves. *Phys.Rev.*, vol. 117, 408-415.
- Hashim, S., Al-Ahbabi, S., Bradley, D.A., Webb, M., Jeynes, C., Ramli, A.T. and Wagiran, H. (2008a). The thermoluminescence response of doped SiO₂ optical fibres subjected to photon and electron irradiations. *Journal of Applied Radiation and Isotopes*, *In press*, doi:10.1016/j.apradiso.2008.06.030.
- Hashim, S., Al-Ahbabi, S., Bradley, D.A., Ramli, A.T., Wagiran, H., Webb, M. and Jeynes, C. (2008b). Determination of dopant concentration of doped SiO₂ optical fibres using ion beam analysis. *17th Annual User Workshop*, Surrey Ion Beam Centre, not published.
- Hashim, S., Bradley, D.A., Saripan, M.I., Ramli, A.T. and Wagiran, H. (2008c). The Thermoluminescence Response of Doped SiO₂ Optical Fibres Subjected to Fast Neutrons. *IRRMA 7 - International Topical Meeting on Industrial Radiation and Radioisotope Measurement Application*. Prague, Czech Republic, submitted for publication.
- Hashim, S., Ramli, A.T, Bradley, D.A. and Wagiran, H. (2006). The thermoluminescence response of Ge-doped optical fibre subjected to proton irradiation. *Proceeding of the 5th National Seminar on Medical Physics 2006*, ISBN 983-43150-4-X, 13-18.

- Hashim, S., Ramli, A.T, Bradley, D.A. and Wagiran, H. (2007). The Thermoluminescence Response of Ge-Doped Optical Fibres to X-Ray Photon Irradiation. *Regional Annual Fundamental Science Seminar 2007 (RAFSS 2007)*, not published.
- Hayes, W. and Jenkin, T.J.L. (1988). Optically detected magnetic resonance studies of exciton trapping by germanium in quartz. *Journal of Physics C: Solid State Physics*, 21, 2391–2398.
- Hendee, W.R. and Ritenour, E.R. (2002). *Medical imaging physics*. 4th edition. USA : John Wiley & Sons Inc.
- Hendee, W.R., Ibbott, G.S. and Hendee, E.G. (2005). *Radiation therapy physics*. 3rd edition. USA : John Wiley & Sons Inc.
- Horowitz, Y. S. (2001). Theory of Thermoluminescence gamma dose response: The unified interaction model. *Nucl. Inst. And Methods in Physics Research B*, vol. 184, 68-84.
- Houston, A.L, Justus, B.L., Falkenstein, P.L., Miller, R.W., Ning, H. and Altemus, R. (2002). Optically stimulated luminescence glass optical fibre dosimeter. *Radiat. Prot. Dosim.*, 101, 23-26.
- <http://www.britannica.com>. (2008). Accessed on 4th August 2008.
- <http://www.thermo.com/rmp>. (2009). Accessed on 17th March 2009.
- ICRU (1976). Determination of absorbed dose in a patient irradiated by beams of x or gamma rays in radiotherapy procedures. ICRU report 24, Bethesda, Maryland.

- ICRU (1998). Fundamental quantities and units for ionizing radiation. ICRU report 86, Bethesda, Maryland.
- Image Processing and Analysis in Java. (2006). Image-J software: <http://rsb.info.nih.gov/ij/docs/index.html>. Accessed on 1st July 2006.
- Johansson, S.A.E and Johansson, T.B. (1976). Analytical application of particle induced X-ray emission. *Nuclear instruments and methods*, 137, 473-516.
- Karmakar, B. (2005). In the land of common glasses. *Science and culture*, 71, 103-115.
- Kaabar, W. (2008). *Bone cartilage interface using PIXE and RBS analysis*. University of Surrey : MPhil / PhD Assessment Report.
- Khanlary, M.R and Townsend, P.D. (1993). Luminescence spectra of germanosilicate optical fibres. II: thermoluminescence. *Journal of Physics D: Applied Physics*, 26, 379 – 386.
- Kirsh, Y., Townsend, J.E. and Townsend, P.D. (1989). Kinetic analysis of the new sensitization effect in the TL of silica optical fibres. *Physica Status Solidi*, 114, 739–747.
- Kivits, P. and Hagebeuk, H.J.L. (1977). *J. Luminescence*, vol. 15, 1.
- Knoll G.F. (2000). *Radiation detection and measurement*. 3rd edition. USA : John Wiley & Sons Inc.
- Kron, T. (1999). Applications of thermoluminescence dosimetry in medicine. *Rad. Prot. Dos.*, 85, 333-340.

- Kurtin, S., Shifrin, G.A. and McGill, J.C. (1969). Ion implantation damage of silicon as observed by optical reflection spectroscopy. *Appl. Phys. Letters*, 14, 223.
- Lapp, R.E. and Andrews, H.L. (1972). *Nuclear Radiation Physics*. 4th edition, New Jersey : Prentice Hall Inc.
- Lushchik, C.H.B. (1956). The investigation of trapping centers in crystals by the method of thermal bleaching. *Soviet Physics, JETP* 3, 390-399.
- Lyytikäinen, K., Huntington, S.T., Carter, A.L.G., McNamara, P., Fleming, S., Abramczyk, J., Kaplin, I. and Schotz, G. (2004). Dopant diffusion during optical fibre drawing. *Optics Express*, vol. 12, 972-977.
- MacChesney, J.B., O'Connor, P.B., DiMarcello, F.V., Simpson, J.R. and Lazay, P.D. (1974). Preparation of low loss optical fibres using simultaneous vapor deposition and fusion, *Proc. 10th Int. Congr. Glass*, Kyoto, Japan.
- MacChesney, J.B., Johnson, J.D.W., Bhandarkar, S., Bohrer, M.P., Fleming, J.W., Monberg, E.M. and Trevor, D.J. (1988). Optical fibres by a hybrid process using sol-gel silica cladding tube. *J. Non-Cryst. Solids*, 226, 232-238.
- MacChesney, J.B. (2000). MCVD: Its origin and subsequent development. *IEEE journal of quantum electronics*, Vol. 6, No. 6, 1305-1306.
- Mahesh, K., Weng, P.S. and Furetta, C. (1989). *Thermoluminescence in solids and its application*. Kent : Nuclear Technology Publishing.
- Mazey, D.J., Nelson, R.S. and Barnes, R.S. (1968). Observation of ion bombardment damage in silicon. *Phil. Mag.*, 17, 1145-1161.

- McKeever, S.W.S., Moscovitch, M. and Townsend, P.D. (1995). *Thermoluminescence Dosimetry Materials: Properties and Uses*, Nuclear Technology Publishing, Kent.
- McKeever, S.W.S and Moscovitch, M. (2003). On the advantages and disadvantages of optically stimulated luminescence dosimetry and thermoluminescence dosimetry. *Rad. Prot. Dos.*, 104, 263-270.
- McKinlay, A.F. (1981). Thermoluminescence Dosimetry. *Medical Physics Handbooks 5*, Adam Hilger Ltd, Bristol.
- McNamara, P., Lyytikainen, K.J., Ryan, T., Kaplin, I.J. and Ringer, S.P. (2004). Germanium-rich “starburst” cores in silica-based optical fibres fabricated by Modified Chemical Vapour Deposition. *Optics Communications*, vol. 230, issues 1-3, 45-53.
- Metcalf, P., Kron, T. and Hoban, P. (1997). *The physics of radiotherapy X-rays from linear accelerators*. England : Medical Physics Publishing.
- Moyer, R.F., McElroy, W.R., O’Brien, J.E. and Chamberlain, C.C. (1983). A surface bolus material for high-energy photon and electron therapy. *Journal of Radiology*, 146, 531-532.
- Nagel, S.R., MacChesney, J.B. and Walker, K.L. (1982). An overview of the Modified Chemical Vapour Deposition (MCVD) process and performance. *IEEE journal of quantum electronics*, Vol. 18, No. 4, 459- 476.
- NE Technology Ltd (1996). *Operators manual for Solaro TLD reader*. version 2.00, Reading, UK.
- Niocholas, K. N., Woods, J. and Brit. J. (1964). *Appl. Phys.*, vol. 15, 783.

Nuclear Data Evaluation Lab (2008). Korean Atomic Energy Research Institute.
<http://atom.kaeri.re.kr/cgi-bin/endfplot.pl>. Accessed on 13th June 2008.

Nuttal, R.H.D and Weil, J.A. (1981a). The magnetic properties of the oxygen-hole aluminum centers in crystalline SiO₂. I. [AlO₄]⁰. *Canadian Journal of Physics*, 59, 1696–1708.

Nuttal R.H.D and Weil J.A. (1981b), The magnetic properties of the oxygen–hole aluminum centers in crystalline SiO₂. II. [AlO₄/H⁺]⁺ and [AlO₄/Li⁺]⁺. *Canadian Journal of Physics*, 59, 1709–1718.

Oberhoffer, M. and Schermann, A. (1981). *Applied thermoluminescence dosimetry*. Bristol : Adam Hilger Ltd.

Oxford Instruments Analytical (2002). Technical briefing : Energy dispersive X-ray microanalysis hardware. Oxford, England.

Oxford Instruments NanoAnalysis (2006). INCAEnergy 25 reasons to choose this solution for EDS on the SEM. Oxford, England.

Pagonis, V., Kitis, G. and Furetta, C. (2006). *Numerical and practical exercises in thermoluminescence*. USA : Springer.

Podgorsak, E.B. (2005). *Radiation oncology physics: A handbook for teacher and students*. Vienna : International Atomic Energy Agency.

Pope, J. (1999). *Medical Physics: Imaging*. Oxford : Heinemann Educational Publishers.

- Portal, G. (1981). Preparation and properties of principal TL products, In: Applied thermoluminescence dosimetry, Oberhoffer, M. and Schermann, A. Bristol : Adam Hilger Ltd., 97-122.
- Ramli, A.T, Bradley, D.A., Hashim, S. and Wagiran, H. (2008). The thermoluminescence response of doped SiO₂ optical fibres subjected to alpha particle irradiation. *Journal of Applied Radiation and Isotopes*, *In press*, doi:10.1016/j.apradiso.2008.06.034.
- Randall, J.T. and Wilkins, M.H.F. (1945). Phosphorescence and electron traps: the study of traps distributions. *Proc. Phys. Soc.*, A 184, 336-407.
- Rassiah, P., Ng, K. H., DeWerd, L. A. and Kunugi, K. (2004). A thermoluminescent dosimetry postal dose inter-comparison of radiation therapy centres in Malaysia. *Australasian Physical & Engineering Sciences in Medicine*, 27, 25-29.
- Rebohle, L., Bovany J.V., Grotzschel, R., Markwitz, A., Schmidt, B., Tyschenko, I.E., Skorupa, W., Frab, H. and Leo, K. (1998). Strong blue and violet photo- and electroluminescence from Ge- and Si-implanted silicon dioxide. *Physica Status Solidi (a)*, 165, 31–35.
- Roberto, B., Adolfo, E., Maurizio, A. and Maurizio, C. (2006). Determination of the response to photons and thermal neutrons of new LiF based TL materials for radiation protection purposes. *IEEE Transactions on Nuclear Science*, 53, 1367-1370.
- Safitri, R., Kamal, A.S.M. and Jaafar, M.S. (2006). Analysis of the glow curve characteristics of Nd doped silica fibre TL dosimeters. *5th National Seminar on Medical Physics*, ISBN 983-43150-4-X, 105-108.

- Shivaramu and Ramprasath, V (2000). Effective atomic numbers for photon energy absorption and energy dependence of some thermoluminescent dosimetric compounds. *Nucl. Inst. And Meth. Phys. Research. B.* vol. 168, 294-304.
- Shojai, A., Reed, G.T. and Jeynes, C. (1992). Diffusion of ion implanted neodymium in silica. *J. Phys. D: Apl. Phys.*, 25, 1280-1283.
- Silsbee, R.H. (1961). Electron Spin Resonance in Neutron-Irradiated Quartz. *Journal of Applied Physics*, 32, 1459-1462.
- Simon, A., Jeynes, C., Webb, R.P., Finnis, R., Tabatabaian, Z., Sellin, P.J., Breese, M.B.H., Fellows, D.F., van den Broek, R. and Gwilliam, R.M. (2004). The new Surrey ion beam analysis facility. *Nuclear Instruments and Methods in Physics Research B*, 219–220, 405–409.
- Song, J., Jonsson, H. and Correles, L.R. (2000). Self-trapped excitons in quartz. *Nuclear Instruments and Methods in Physics Research B*, 166–167, 451–458.
- Taggart M. (2007). Surveying the Thermal Neutron Capture Flux via Activation Analysis. University of Surrey : MSc Dissertation.
- Trukhin, A.N., Jansons, J.L. and Truhins, K. (2004). Luminescence of silica glass containing aluminium oxide. *Journal of Non-Crystalline Solids*, 347, 80-86.
- Tsai, T.E., Griscom, D.L. and Friebele, E.J. (1988). Mechanism of intrinsic Si E'-center photogeneration in high purity silica. *Physical Review Letters*, 61, 444–446.

- Warren, W.L., Poindexter, E.H, Oenberg, M. and Müller-Warmuth W. (1992). Paramagnetic Point Defects in Amorphous Silicon Dioxide and Amorphous Silicon Nitride Thin Films. I. a-SiO₂. *Journal of Electrochemical Society*, 139, 872-880.
- Webb, R.P. (1986). Surrey University sputter profile from energy deposition programme. VG software package.
- Wood, D.L., Walker, K.L., Simpson, J.R., MacChesney, J.B., Nash, D.L. and Anguiera, P. (1981). Chemistry of the MCVD process for making optical fibres, 7th *Eur. Conf. Optical Communication*.
- Yan, M.F., MacChesney, J.B., Nagel, S.R. and Rhodes, W.W. (1980). Sintering and optical waveguide glasses. *J. Mater. Sci.*, 15, 1371-1378.
- Yu, K.N., Yip, C.W.Y., Nikezic, D., Ho, J.P.Y. and Koo, V.S.Y. (2003). Comparison among alpha particle energy losses in air obtained from data of SRIM, ICRU and experiments. *Appl. Radiat. and Isot.*, 59, 363-366.
- Yusoff, A.L. (2005a). *Development of silica-based thermoluminescence dosimeters*. University of Exeter : PhD Thesis.
- Yusoff, A.L., Hugtenburg, R.P. and Bradley, D.A. (2005b). Review of development of a silica-based thermoluminescence dosimeter. *Rad. Phys. Chem.*, 74, 459-481.
- Ziegler J.F. (1999). The stopping of energetic light ions in elemental matter. *J.Appl. Phys.*, 85, 1249-1272.
- Ziegler J.F. (2003). SRIM 2003 program : The stopping and range of ions in matter, version 2003. www.srim.org.